VERY EFFICIENT PLASMA GENERATION BY WHISTLER WAVES NEAR THE LOWER HYBRID FREQUENCY

R. W. BOSWELL

Plasma Research Laboratory, Research School of Physical Sciences, The Australian National University, Canberra, ACT, 2601, Australia

Abstract—Experimental results are presented which show that r.f. power at frequencies near the lower hybrid frequency couples resonantly into a standing whistler wave. For an input power flux of less than 5 W cm^{-2} densities above 10^{12} cm^{-3} with close to 100% ionization have been achieved. Measured density, temperatures and wave fields are presented and are used as input parameters for a theoretical model.

1. INTRODUCTION

IT HAS been long known that it is possible to ionize a gas by radio frequency power using either inductive or capacitive coupling methods. Rather than simply relying on the large oscillatory electric fields of the antenna to accelerate electrons to ionizing energies, several resonant excitation methods have been found to be more effective. These often operate at microwave frequencies and typically use some form of slow wave structure such as that described by LISITANO et al. (1970). Recently, interest has been shown in coupling energy into magnetoplasmas at or near the lower hybrid frequency. This interest has been spurred by the desire to heat the ions in toroidal plasma devices where the radial variation of the magnetic field allows the propagation of lower hybrid waves along resonance cones to penetrate into the centre of the plasma. In this paper we describe a technique for producing essentially fully ionized plasma which uses a special antenna structure to couple into a whistler mode wave propagating near the lower hybrid frequency. Average electron densities $\sim 10^{12} \text{ cm}^{-3}$ have been obtained in a 10 cm diameter plasma with an initial filling pressure $\sim 10^{-3}$ torr using much lower r.f. powers and corresponding fluxes of 5 W cm^{-2}. For comparison, the experiment of MOTLEY et al. (1979) involved fluxes of up to several kilowatts cm^{-2}. We have in fact recently demonstrated (BOSWELL et al., 1982) that in a 5 cm diameter magnetoplasma, central densities approaching 10^{14} cm^{-3} are readily achieved in steady state operation using the method described here; however, in the latter case the electron temperature was 3 eV compared with 10 eV for the plasma described by MOTLEY et al. (1979). In this type of discharge one of the main power losses is by electron heat conduction along the magnetic field, so that in a linear device, once the plasma is fully ionized, the effect of increasing the r.f. power is to heat the electrons, the equilibrium temperature being determined primarily by the rapid end losses.

At frequencies higher than the lower hybrid frequency, MOTLEY et al. (1979) report a significantly improved performance approaching that of the source described here. However, our main interest here is r.f. excitation near the lower hybrid frequency and not excitation of an "overdense" plasma column.

Using a higher filling pressure $\sim 4 \times 10^{-2}$ torr, LEHANE and THONEMANN (1965) have obtained a 10 cm diameter plasma with density $\sim 10^{13} \text{ cm}^{-3}$ generated by inductively coupled r.f. at a power flux of about 50 W cm^{-2}. The plasma was, however,

only 1% ionized. Generally speaking, the absence of detailed measurements has made it difficult to compare the results of the various resonant coupling methods with theoretical models. In this paper we show the actual mode structure of the wave responsible for the resonant coupling, and describe a theoretical model which yields dispersion and damping of the wave in quite good agreement with the experimental values. The general principles of the coupling mechanism are discussed in Section 2 of the paper which is followed by a description of the apparatus in Section 3. The magnetic probe and density measurements are described in Section 4 and compared with theory in Section 5. A discussion of the power balance including ionization and loss rates is given in Section 6 with the conclusions following in Section 7.

2. METHOD OF RESONANT COUPLING

The primary aim of the experiment is to couple r.f. energy into the centre of a magnetoplasma and have the energy transferred to the plasma particles. The intention therefore must be to excite an eigenmode of the plasma which has maximum power dissipation (determined by $\eta|j|^2$) in the centre. Here we wish to emphasize that we do not wish to excite electrostatic "lower hybrid" waves which propagate into the plasma along a resonance cone, but rather a mode which is basically a waveguide or body mode of the plasma.

For the experiment described below, we have chosen a frequency range $\Omega_i \ll \omega \ll \Omega_e \ll \omega_{pe}$ for the r.f., where Ω_i and Ω_e are the ion and electron gyro frequencies and ω_{pe} is the electron plasma frequency. This choice is dictated both by experimental convenience and for simplicity in theoretical interpretation. To obtain the radial distribution of the fields and currents for waves which propagate in this frequency range we need retain only the Hall term in the Ohm's Law

$$E = \frac{1}{n_e}\mathbf{j} \times \mathbf{B}. \tag{1}$$

Combining this with Maxwell's equations, we arrive at the plane wave dispersion relation

$$q^2 = \frac{\omega\,\omega_{pe}}{\Omega_e c^2 \cos \alpha} \tag{2}$$

where the wave vector $\mathbf{q}$ makes an angle α with the axial magnetic field B_0 and $q^2 = k^2 + \gamma^2$, k and γ being parallel and perpendicular wave numbers respectively. In order to clearly illustrate the various eigen modes of the cylindrical plasma we shall take perfectly conducting boundaries which allow solutions in the zero resistivity case considered here. Consequently the boundary conditions require that the tangential components of the wave electric fields are zero and we can derive the dispersion relation for the cylindrical eigenmodes (DAVIES, 1970),

$$\frac{mq}{a} J_m(\gamma a) + \gamma k J'_m(\gamma a) = 0 \tag{3}$$

where field quantities are assumed to vary as $f(r) \exp i(\omega t - kz - m\theta)$, m is the azimuthal mode number, a is the plasma radius and J is an mth order Bessel function of the first kind.
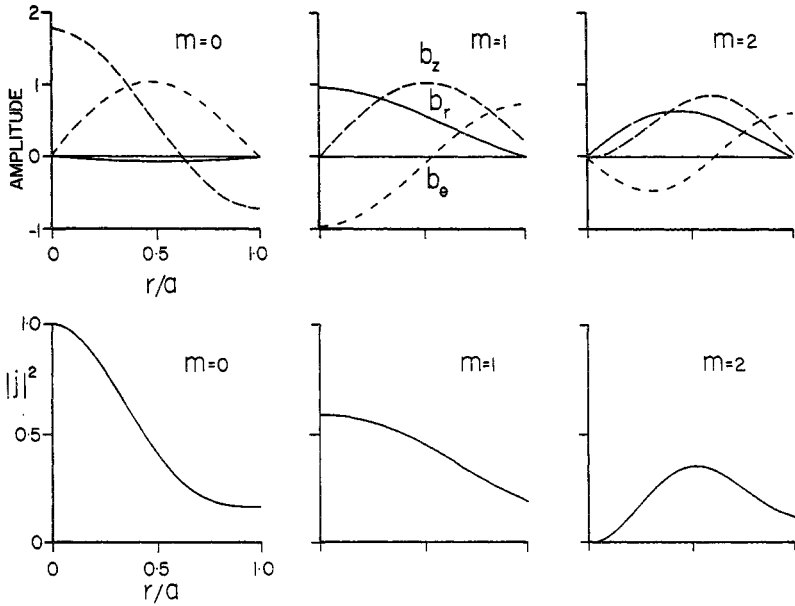

FIG. 1.—Radial variation of the wave fields and $|j|^2$ for azimuthal mode numbers $m = 0, 1, 2$ with the simplest radial mode number.
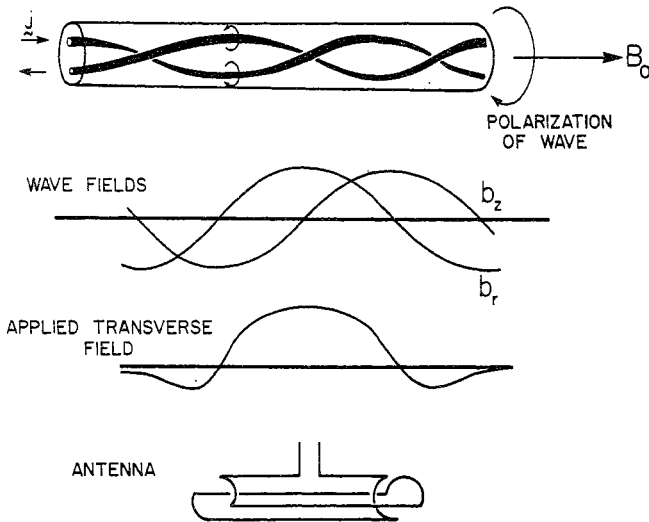

FIG. 2.—Sketch of the current system for an $m = 1$ helicon with associated wave fields (a, b). The exciting antenna and its applied transverse field are shown in c and d.

The wave fields for $m = 0, m = 1$ and $m = 2$ are plotted in Fig. 1 for the most simple $n = 1$ radial mode. Also plotted is $|j|^2$ to give an idea of the power density within the wave and hence the region of greatest dissipation. As can be seen only the $m = 0$ and $m = 1$ modes have maximum power density in the centre. However, the $m = 0$ mode is axisymmetric and can most effectively be launched by an antenna actually in the centre of the plasma whereas we wish to excite the waves externally. A sketch of the remaining mode, the $m = 1$, is shown in Fig. 2a which represents a snapshot of the wave fields. Essentially, the wave can be imagined as a twisted bifilar current system, the pitch of the twist being the wavelength. The important thing to notice is that the wave magnetic field in the centre is purely transverse and rotates in time. It would therefore be possible to excite the wave using a rotating field, as suggested by BLEVEN and THONEMANN (1962) by using a set of loop antennae outside the plasma excited in the correct phase. However, as the only polarization which can propagate is the $m = 1$ (the $m = -1$ being evanescent for this frequency range) a linearly polarized transverse r.f. field can be applied by using two loop antennae and allowing the plasma to automatically select the correct polarization. This is illustrated in Figs. 2(b) and (c) where the axial variation of the transverse field generated by the double loop antenna shown in Fig. 2(d) can be seen to closely resemble the axial variation of the radial magnetic field of the wave. Experimental measurements of the wave fields described later show this simple model to be qualitatively correct.

3. EXPERIMENTAL ARRANGEMENT

The general layout of the apparatus is shown in Fig. 3. A diameter of 10 cm was chosen for the vacuum vessel to allow probe measurements to be taken of the wave fields in the plasma. Measurements made in a smaller, 5 cm diameter vessel were highly distorted due to the plasma being significantly perturbed by the probes. To minimize filling pressure gradients, the 120 cm long Pyrex vessel was pumped through the same end as the gas inlet. The base pressure was $1-3 \times 10^{-6}$ torr of argon. An
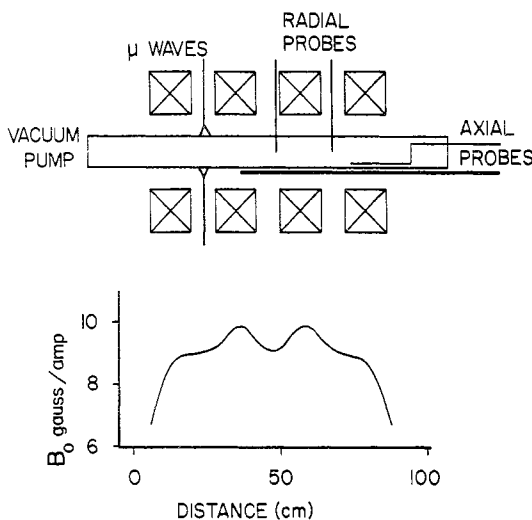

FIG. 3.—Experimental arrangement.

axial magnetic field was generated by a solenoid consisting of four identical coils, 15 cm wide with inner and outer diameters 25 and 55 cm respectively. With an axial separation between the coils of 15 cm the solenoid produced a field of about 10 G amp^{-1} uniform to $+5\%$ on axis (see Fig. 3). The maximum field was 1.6 kG.

The magnetic field probes consisted of single layer solenoidal coils, 2 mm in diameter and 6 mm long. The coils were centre tapped and had approximately 50 windings. The radial b_r and azimuthal b_θ wave fields were measured with probes inserted through the radial ports in the vacuum vessel, and the axial b_z component with a probe which could move axially along the cylinder but with a dog-leg in it to allow radial variation. The axial variations of the wave fields were measured by moving the small coils along the outside of the vacuum vessel parallel to the axis. The orientation of the probes relative to the r.f. antenna allowed only b_r and b_z to be measured. The probes were calibrated relative to each other by inserting them into a transmission line which produced a very uniform field from a known current source. The maximum wave fields ~ 1 G were obtained for $B_0 \sim$ kG and therefore presented a very small perturbation, consistent with the linearized dispersion relation discussed later.

A floating plane double Langmuir probe with a dog-leg bend was inserted through the end plate of the vessel and used to make relative measurements of the plasma density and electron temperature. The probe was oriented parallel to B_0 so that the electron and ion currents could flow along field lines direct to the probe collection areas.

Measurements of the electron temperature and radial density profile have been made in a broadly similar plasma by BROWN et al. (1971) using a Langmuir probe calibrated against a microwave interferometer. A similar method has been used here where the electron temperature and relative plasma density were measured by moving the floating probe radially across the plasma. Absolute measurements of the electron density were made with a conventional 8 mm microwave interferometer. The radial profiles were approximated by a fifth order polynomial fit and the average density calculated numerically. For reasonably uniform plasmas, this procedure gives quite accurate measurements of the electron density; however, for the highly peaked distributions measured at $B_0 > 750$ G, the short path length through the plasma and refraction of the microwaves from the central core plasma introduced errors of about $\pm 50\%$.

The choice of coupling to a whistler mode imposes certain constraints on the excitation frequency and antenna wavelength which are limited through the dispersion relation. For simplicity let us consider the plane wave dispersion and set $\alpha = 0$ in equation 2, yielding

$$\lambda = \left(\frac{\Omega_e}{\omega}\right)^{\frac{1}{2}} \frac{2\pi c}{\omega_{pe}}$$

which simplifies to

$$\lambda \sim 5 \times 10^9 \left(\frac{B_0}{nf}\right)^{\frac{1}{2}} \text{ cm}$$

where B_0 is in gauss, n in cm^{-3} and f in Hertz. In the experiment $f = 8.6$ MHz, hence

$$\lambda \sim 1.7 \times 10^6 \left(\frac{B_0}{n} \right)^{\frac{1}{2}}. \tag{4}$$

The optimal wavelength is clearly linked to the electron density and B_0 through equation (4) which can be regarded as a resonance condition. Empirically, we found that best results over the whole range of B were obtained with an antenna length of 25 cm, which was found to couple best to waves with $\lambda = 50$ cm. However, as can be seen from equation (4), the density must increase with B_0 if the resonance condition is to remain satisfied. In the next section this is shown to hold reasonably well. Antennae of other lengths were also tried but they did not provide good coupling for high B_0 and did not satisfy the resonance condition. All results presented below were taken with an antenna length of 25 cm.

The r.f. power at 8.8 MHz was supplied from an oscillator–amplifier system which effectively decoupled the oscillator from the plasma thereby preventing frequency "pulling" on the oscillator by impedance changes in the plasma load. The power was delivered to the plasma by a coaxial cable and matched into the antenna with two high voltage variable capacitors arranged in a π network (see Fig. 4). In operation, the lower value capacitor tuned the l.c. circuit to resonate with the oscillator and the other larger capacitor served to match the resonant circuit to the coaxial cable. A half-wavelength section of coaxial cable was connected across the antenna inductance to improve the matching between the unbalanced coaxial line and the balanced antenna. The power delivered into the resonant circuit was measured to be 180 ± 20 W and was kept at this level throughout the experiment. As the standing wave ratio was close to unity and the components of the resonant circuit did not warm up, it is reasonable to assume that virtualy all the power was delivered to the plasma. To minimize damage to the probes, the r.f. supply was pulsed at 10 Hz with a 10% duty cycle.
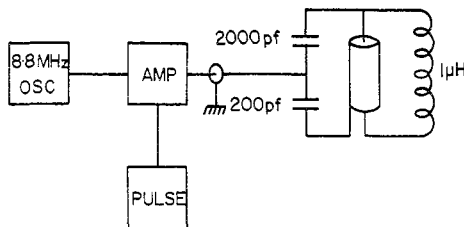

Fig. 4.—RF coupling circuit.

4. EXPERIMENTAL RESULTS

The experiment was conducted at fixed frequency (8.8 MHz) and power (180 W); the antenna length was 25 cm, the filling gas argon at 1.5×10^{-3} torr and the magnetic field B_0 was increased systematically up to its maximum value of 1500 G. The radial and axial variation of the wave fields and the electron temperature and density were all measured as a function of B_0.

The radial dependence of b_r, b_θ and b_z is shown in Fig. 5(a), (b) and (c) for $B_0 = 33$ G. The experimental measurements show that the aximuthal mode is $m = 1$ for the lowest radial mode number $n = 1$. By comparing signals from probes spaced 90° apart
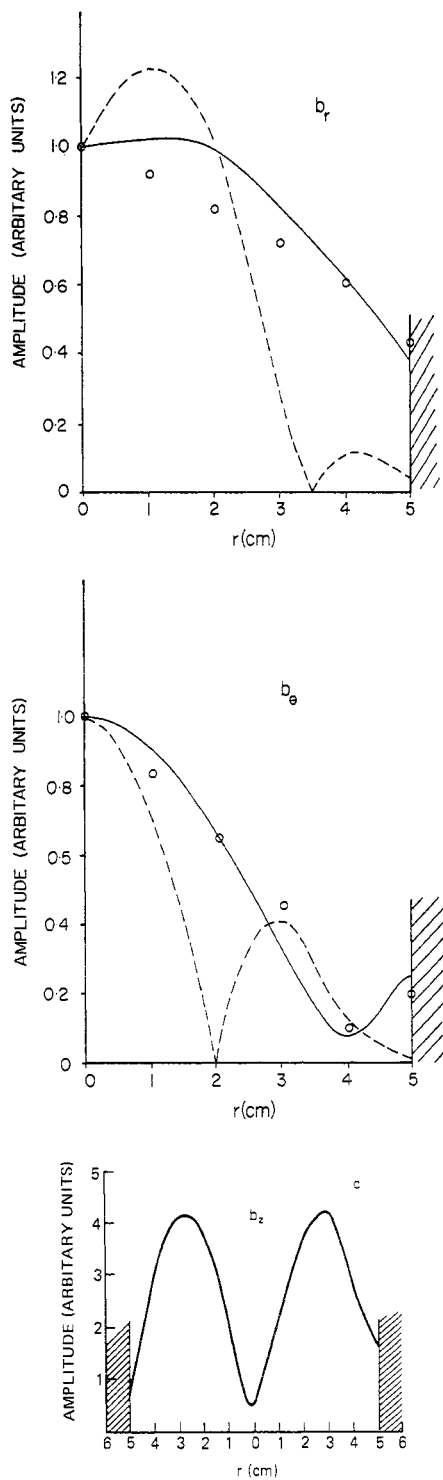
FIG. 5.—Radial variation of the components of the wave fields, b_r, b_θ and b_z for $B = 33$ G. The solid curve for b_r and b_θ is a theoretical fit for $ak = 0.63$ and $\Omega_e\tau = 3$; the broken curve has $\Omega_e\tau = 300$.
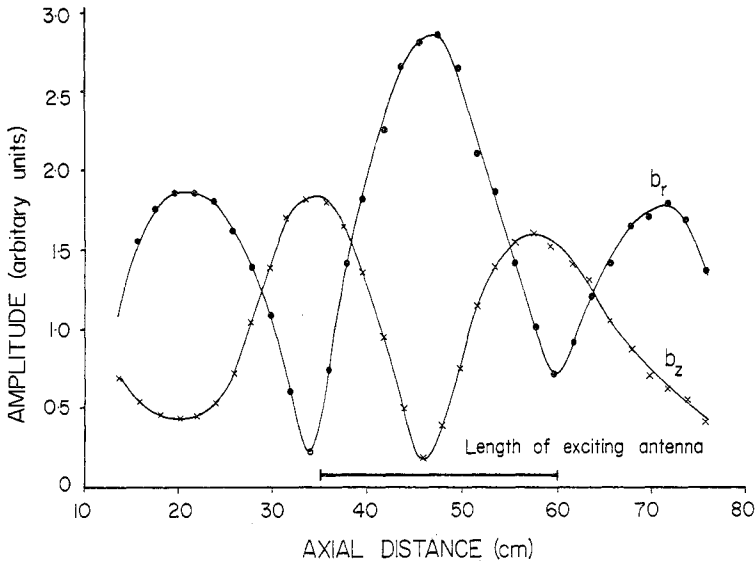
Fig. 6.—Axial variation of b_r and b_z for $B_0 \sim 100$ G. At each minimum of the wave fields there is a phase change of $180°$.

azimuthally, the polarization of the wave was measured and found to be in the same direction as the electron gyro rotation, i.e. right-handed. The solid and broken lines in Fig. 5(a) and (b) are theoretical fits to the experimental points for different values of the resistivity. This will be discussed in greater detail below. The axial wavelength was determined by measuring the axial variation of the b_r and b_z components of the wavefields outside the plasma along the central 90 cm of the vacuum vessel. A good example of one of these plots is shown in Fig. 6 for $B_0 = 100$ G. The uncertainty in the measured amplitude of b_z was about $\pm 5\%$ and of b_r about $\pm 10\%$ due mainly to alignment difficulties and electrostatic pick-up from the antenna. Each minimum in the wave field has an associated phase change of $180°$ showing quite clearly that a standing wave was being excited. There is a clear correlation between the position and amplitude of the field component b_r and the position of the antenna.

At weak magnetic fields, the density remained constant around 10^{11} cm^{-3}. The electron temperature remained constant at 2.7 ± 0.3 eV for all values of B_0. If these values of B_0 ($= 100$ G) and density ($= 10^{11}$ cm^{-3}) are inserted into equation (4) we find that the resonance condition is reasonably well satisfied. As B_0 increases, the coupling becomes less ideal although the mode structure remains the same. For these low values of B_0, the ionization is by electrons accelerated directly by the electric fields of the antenna. An $m = 1$ standing whistler wave is launched by the antenna but the wave plays little role in the plasma production. The discharge colour is light pink arising from the many lines of neutral argon (ArI) in the red part of the spectrum.

The plasma density remains approximately constant $\sim 10^{11}$ cm^{-3} until B_0 is increased to ~ 500 G, at which point the plasma switches suddenly into a new mode, in which the electron density is five times greater and the central volume of the plasma turns light blue due to emission of ArII lines. The radial profiles of the electron density and the wave fields become more peaked and the axial wavelength doubles. As B_0
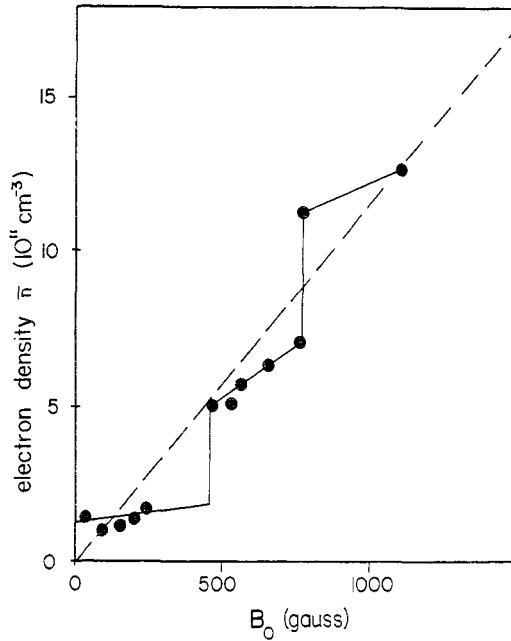
Fig. 7.—Variation of the average electron density $\bar{n}$ with B_0. The solid curve is fitted to the experimental points and the broken curve is for plane wave whistler propagation.

is further increased the measured wavelength slowly decreases and the density increases until at 750 G the density again suddenly increases by a factor of two accompanied by further changes in the wave fields and wavelength. In this mode the plasma has a very peaked density distribution and a bright blue central core. The b_r and b_θ field components are an order of magnitude greater than b_z and have maximum amplitudes of approximately 1 G.

The variation of the average electron density $\bar{n}$ determined by the interferometer and the Langmuir probe is shown in Fig. 7 as a function of B_0. The wavelengths measured at the corresponding magnetic fields are shown in Fig. 8. As can be seen from Fig. 6, the wavelength is not constant along the axis: in this rather ideal example there is a 20% variation although the matching between the antenna length and the plasma wavelength is almost perfect. For whistler wavelengths much shorter than that imposed by the antenna there are variations of greater than 50% along the axis. The wavelengths given in Fig. 8 are those measured under the antenna. The wave in the plasma is clearly a forced oscillation and, as mentioned earlier, the antenna length was chosen empirically to provide the best coupling. For other antenna lengths, whether too short or too long the sudden plasma density jumps did not occur and the density remained reasonably constant as B_0 was changed. The solid line in Fig. 7 is fitted to the experimental points and the broken line is the simple dispersion relation mentioned earlier for plane whistler waves of wavelength 50 cm, which in this case reduces to:
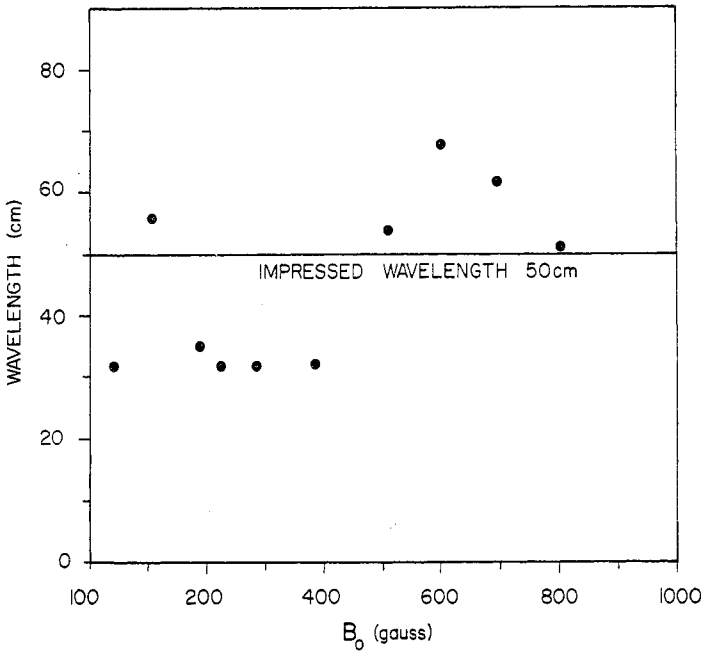
$$\bar{n} = 1.2 \times 10^9 \ B_0 \ cm^{-3}.$$

FIG. 8.—Measured wavelength under the antenna as a function of B_0.

For $B < 500$ G, the only field where the resonance condition is well satisfied is $B_0 \sim 100$ G for which the measured wavelength is 55 cm. Away from this ideal matching the wavelength remains at about 2/3 of the matched wavelength and the coupling is basically via a forced oscillation. However, at around 500 G, the density increases, the wavelength reverts to that of the impressed wavelength and the simple dispersion relation is once again satisfied. Essentially the same thing happens around 750 G but in this case the greater variation of the radial density profile makes the simple dispersion relation rather inaccurate.

Radial profiles of the wave fields are shown in Fig. 9. They clearly represent an $m = 1$, $n = 1$ mode up to $B_0 = 758$ G where the second density jump occurs. The last two profiles at $B_0 = 800$ and 1130 G may represent $m = 1$, $n = 2$. The shift of the maximum amplitude away from the centre of the plasma is caused by the presence of the probe, since the whole central blue core of the plasma can be seen to move away from the probe. Electron density profiles taken at essentially the same B_0 as the wave field profiles are shown in Fig. 10. It should be remembered at this point that the r.f. input power for all values of B_0 was kept constant at 180 W. The increase in density with B_0 could only result from efficient coupling of energy to the whistler wave and consequent transfer of wave energy to the plasma. For weak fields $B_0 \sim 33$ G the density profile is approximately parabolic, but as B_0 is increased, the density profiles become very similar to those of the wave fields, suggesting that it is ohmic dissipation of the wave energy proportional to $n|j|^2$ that is maintaining the plasma.
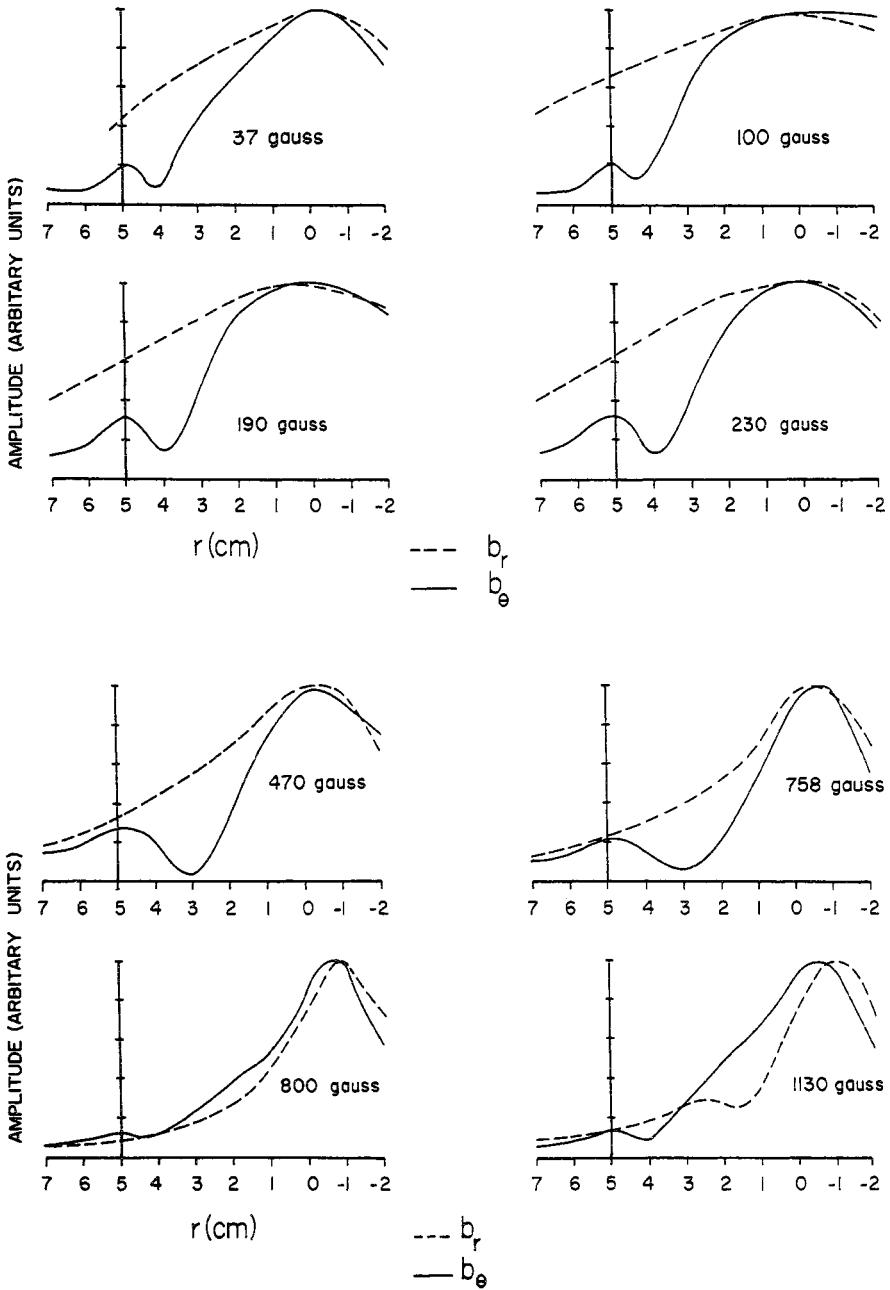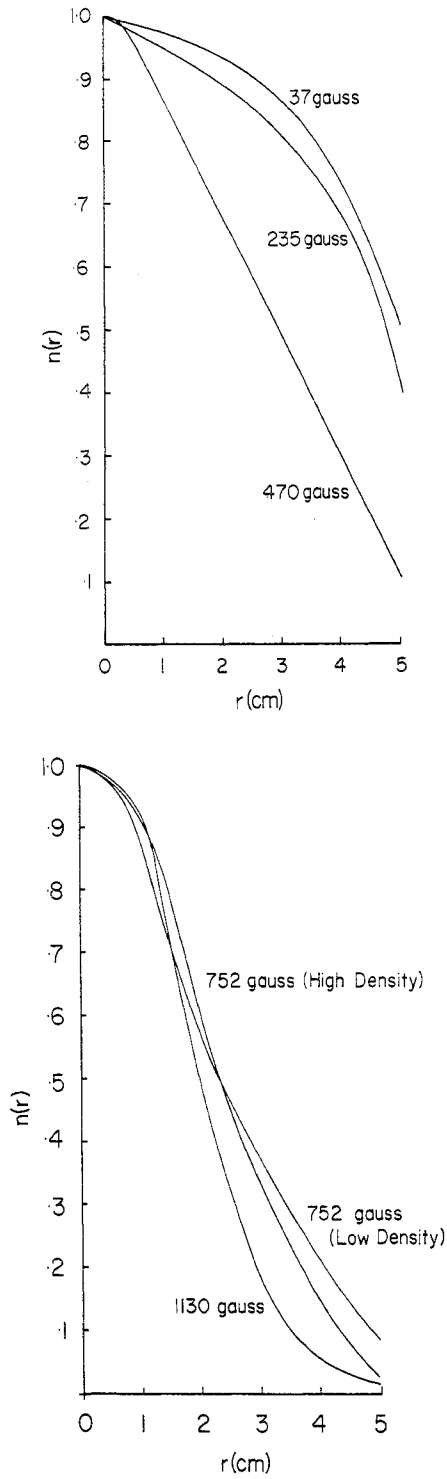
FIG. 9.—Radial variation of b_r and b_θ for various B_0.

FIG. 10.—Polynomial fits to the measured radial density profiles for a number of B_0 values.

5. MODELLING OF THE WAVE EXCITATION

Since we have now shown experimentally that the wave is an $m = 1$, $n = 1$ whistler, it should be possible to theoretically model the dispersion. For this we use Ohm's law including resistivity, the Hall term, and electron inertia but assume ions are immobile.

$$E = \eta\mathbf{j} + \frac{1}{ne}\mathbf{j} \times \mathbf{B} + \frac{1}{ne^2}\frac{\partial \mathbf{j}}{\partial t}.$$

A numerical method for solving this equation when the electron density was a function of radius was developed by DAVIES and CHRISTIANSEN (1969) and modified by BOSWELL (1983) to include the effects of rigid non-conducting cylindrical boundaries. An initial problem was that of resistivity, since in trying to fit the radial wave profiles shown in Fig. 5 it was found that the effective collision frequency had to be at least 1000 times greater than the theoretical value. Using the theoretical value produced large fields in a very narrow layer at the surface of the plasma which propagated into the plasma a distance of about the skin depth. This difficulty always arises when trying to solve eigenmode problems for "abrupt vacuum interfaces" in low resistivity magnetoplasmas, but not when I currents are allowed to flow in a perfectly conducting boundary in intimate contact with the plasma. The discrepancy between experiment and theory would be resolved if we are prepared to accept either that the glass walls
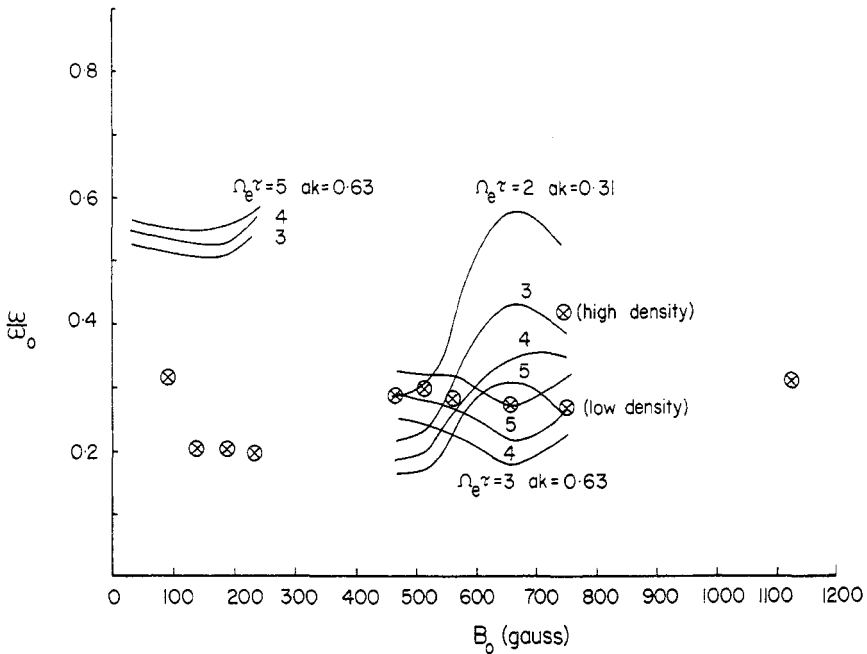

FIG. 11.—X experimental points. The solid lines are theoretical fits for values of $ak = 0.63$ and 0.31 for various values of $\Omega_e\tau$.

themselves become conducting in the presence of the plasma or that an adequately conducting layer is formed on their inner surface.

The alternative is to seek solutions in which the conductivity is allowed to take values which fit the experimental wave profiles, but are less than those deduced on the basis of binary collisions, leaving aside for the moment the physical justification for using such phenomenological values. For the case under consideration here, this second alternative seems to have the greater physical justification.

The plasma was modelled in a self-consistent manner by keeping the frequency constant and the wavelength equal to the antenna wavelength. For each value of B_0, the measured values of the radial variation and average density were inserted into the program and solutions of complex ω sought which were closest to the experimental values. Various theoretical fits to the experimental points are shown in Fig. 11. A very good fit was found with B_0 between 500 and 750 G for values of $\Omega_e \tau \sim 3$–5. For $B_0 > 750$ G the very steep radial density gradients produced severe numerical errors and no reliable solutions could be found. The fit for low values of B_0 is less good but is nevertheless within a factor of two. The region of optimum coupling is actually centred on the lower hybrid frequency.

6. DISCUSSION

For fields $B_0 > 750$ G, the spectroscopic measurements show that the emission from the central blue core of the plasma consists of ArII (Ar^+) lines, primarily 4806 and 4880 Å. Surrounding the core is an annulus of ArI emission, with very little ArI emission coming from the core, suggesting that the core is essentially fully ionized. The discrepancy between the central density $\sim 5 \times 10^{12}$ cm^{-3} (the central density is about four times the average for $B_0 > 750$ G) and the filling density of 5×10^{13} cm^{-3} can be easily accounted for. In this type of discharge, the neutral gas temperature reaches about 3000 K in the steady state (BOSWELL et al., 1982). Since we require pressure balance between the cold (300°K) gas at either end of the discharge tube and the hot gas inside the discharge, the equilibrium number density of neutrals in the discharge is an order of magnitude lower than the original filling pressure would suggest. This phenomenon, which commonly occurs in pulsed gas lasers, is called gas pumping. Consequently, although the average plasma density across the full cross-section represents a 20% ionization, the central plasma is fully ionized.

It is now possible to determine the equilibrium conditions of the plasma. The ion neutral collision mean path is much longer than the discharge so the magnetic field will constrain the plasma to flow along the axis of the discharge and out of the ends. The axial drift velocity is determined by the ambipolar flow and since $T_i \ll T_e$, is given by $C_s = (k_B T_e/m_i)^{\frac{1}{2}}$ where T_i and T_e are the ion and electron temperatures. In equilibrium, the loss rate of (singly) ionized ions from the ends must equal the generation rate:

$$2\bar{n}A\left(\frac{k_B T_e}{m_i}\right)^{\frac{1}{2}} = n_0\bar{n}(\sigma v)_i Al$$

where A is the cross-sectional area of the plasma of length l and $(\sigma v)_i$ is the rate coefficient for electron ionization of the argon gas with density n_0. We assume in this simple model that there are very few doubly ionized argon ions in the discharge

and that recombination only occurs at the ends. We have mentioned in Section 5 that the plasma density profiles closely resemble the dissipation profiles for the whistler waves. The r.f. input power is coupled into the waves which then transfers it to the plasma electrons. The energy is subsequently dissipated by ionization and excitation, and by energy flow to the ends of the discharge. Hence for equilibrium we have

$$P = n_0 \bar{n} (\sigma v)_i E A l + \frac{3}{2} \bar{\gamma} k_B T_e C_s 2 A$$

where E is the average energy required to produce an electron ion pair, and electrons with energy greater than the plasma potential carry away $3/2 \, \gamma \bar{n} k_B T_e$ average energy at a speed C_s through the area $2A$ (since the plasma has two ends). The factor γ is given by MOTLEY et al. (1975) for a collisional plasma as:

$$\gamma = \frac{1}{3} \left[4 + \ln \left(\frac{m_i / 2\pi m_e}{1 + 5 T_i / 3 T_e} \right) \right]$$
$$\sim 4.5.$$

The collisional aspects of the plasma will be discussed below. Inserting the experimental values into this equation, we find for $B_0 > 750$ G that the power loss due to escaping electrons is ~ 100 W. Since $P = 180 \pm 20$ W, we can only balance the equation by taking E to be the ionization energy of 15.7 eV.

   We have shown in Section 4 that to fit the theoretical dispersion to the experimental measurements, a value of $\Omega_e \tau$ between 3 and 5 was required over a wide range of B_0. This implies a collision frequency for the electrons at least 10^3 times greater than Coulomb collisions which suggest that plasma instabilities are playing a major role in the energy transfer mechanism and thermalization of the electrons.

   Although we have not investigated this matter in any detail, an heuristic argument can be presented which accounts for most of the observations. Taking once again $B_0 \sim 1$ kG, the maximum wave amplitude was of the order of 1 G, implying that the maximum wave electric fields were about 1 kV m^{-1}. Since the wave is stationary, the plasma electrons will oscillate in the potential wells and in the absence of a scattering mechanism, will have no nett gain in energy. However, at some time their drift velocity v_D must become greater than their thermal velocity v_T and the electron–ion two stream or Buneman instability can occur. Since the laboratory frame is essentially the ion frame we obtain for an instability with

$$\omega \ll \omega_{pe} : \omega \sim 0.8 \, \omega_{pe} \left(\frac{m_e}{m_i} \right)^{1/3} \quad \text{and a growth rate } \gamma \sim \omega_{pe} \left(\frac{m_e}{m_i} \right)^{1/3}.$$

For the argon plasma considered here $(m_e/m_i)^{1/3} = 2.4 \times 10^{-2}$ and taking the average density for $B_0 = 1$ kG of $\bar{n} = 10^{12}$ cm^{-3} we obtain for the instability $\omega = 1.2 \times 10^9$ s^{-1} with a comparable growth rate.

   This is considerably higher than the Coulomb collision frequency and yields a value of $\Omega_e \tau \sim 15$ which is quite close to the value required by the dispersion theory. It is now quite easy to understand how the wave transfers its energy to the electrons.

If the electrons are scattered at a rate determined by the instability, they have about 100 collisions per whistler wave period and consequently would be accelerated by the quasi-static electric field experienced between collisions. The steady state equilibrium would presumably involve a sufficient level of turbulence to scatter the collective motion of the electrons in the whistler wave fields and maintain a Maxwellian distribution. We are presently investigating this problem using a much higher r.f. power and the results will be presented in a later publication.

7. CONCLUSIONS

By using a double loop antenna which produces an oscillating transverse magnetic field we have shown that it is possible to launch an $m = 1$ whistler wave in a weakly ionized cylindrical magnetoplasma. As the steady axial magnetic field B_0 is increased, the density of the plasma increases in a stepwise manner so as to keep the plasma wavelength approximately equal to the antenna wavelength. For $B_0 \sim 1$ kilogauss the central core of the plasma is virtually completely ionized with the optical emissions being typical of ArII, the ArI emission coming from an annulus around this core. The coupling of the RF power to the plasma is essentially 100% efficient with about 50% of the power being lost out of the ends of the discharge and 50% going into ionization and excitation. The strong coupling of the whistler wave to the plasma could only be explained by invoking a collision frequency more than 1000 times greater than the Coulomb collision frequency. A possible mechanism to explain this anomaly would be the Buneman instability generated by electrons accelerated by the strong fields of the whistler wave.

REFERENCES

BLEVIN H. A. and THONEMANN P. C. (1965) *Proc. phys. Soc.* **85**, 301.
BOSWELL R. W., PORTEOUS R. K., PRYTZ A., BOUCHOULE A. and RANSON P. (1982) *Phys. Letts.* **91A**, 163.
BOSWELL R. W. (1983) Submitted for publication.
BROWN I. G., COMPHER A. B. and KUNKEL W. B. (1971) *Physics Fluids* **14**, 1377.
DAVIES B. J. (1970) *Plasma Physics* **4**, 43.
DAVIES B. and CHRISTIANSEN P. J. (1969) *Plasma Physics* **11**, 987.
LEHANE J. A. and THONEMANN P. C. (1965) *Proc. Soc.* **85**, 301.
LISITANO G., ELLIS R. A., HOOKE W. M. and STIX T. H. (1970) *Rev. Sci. Inst.* **41**, 600.
MOTLEY R. W., BERNABEI S., HOOKE W. M. and JASSBY D. L. (1975) *J. appl Phys.* **46**, 3286.
MOTLEY R. W., BERNABEI S. and HOOKE W. M. (1979) *Rev. scient. Instrum.* **50**, 1586.